
MOMENTUM-SAM: SHARPNESS AWARE MINIMIZATION WITHOUT COMPUTATIONAL OVERHEAD

Marlon Becker **Frederick Altrock** **Benjamin Risse**
Department for Computer Science & Institute for Geoinformatics
University of Muenster, Germany
{marlonbecker, f.altrock, b.risse}@uni-muenster.de

ABSTRACT

The recently proposed optimization algorithm for deep neural networks Sharpness Aware Minimization (SAM) suggests perturbing parameters before gradient calculation by a gradient ascent step to guide the optimization into parameter space regions of flat loss. While significant generalization improvements and thus reduction of overfitting could be demonstrated, the computational costs are doubled due to the additionally needed gradient calculation, making SAM unfeasible in case of limited computationally capacities. Motivated by Nesterov Accelerated Gradient (NAG) we propose Momentum-SAM (MSAM), which perturbs parameters in the direction of the accumulated momentum vector to achieve low sharpness without significant computational overhead or memory demands over SGD or Adam. We evaluate MSAM in detail and reveal insights on separable mechanisms of NAG, SAM and MSAM regarding training optimization and generalization. Code is available at <https://github.com/MarlonBecker/MSAM>.

1 INTRODUCTION

While artificial neural networks (ANNs) are typically trained by Empirical Risk Minimization (ERM), i.e., the minimization of a predefined loss function on a finite set of training data, the actual purpose is to generalize over this dataset and fit the model to the underlying data distribution. Due to heavy overparameterization of state-of-the-art ANN models (Nakkiran et al., 2021), the risk of assimilating the training data increases. As a consequence, a fundamental challenge in designing network architectures and training procedures is to ensure the objective of ERM to be an adequate proxy for learning the underlying data distribution.

One strategy to tackle this problem is to exploit the properties of the loss landscape of the parameter space on the training data. A strong link between the sharpness in this loss landscape and the models generalization capability has been proposed by Hochreiter & Schmidhuber (1994) and further analyzed in the work of Keskar et al. (2017). Following these works, Foret et al. (2021) proposed an algorithm to explicitly reduce the sharpness of loss minima and thereby improve the generalization performance, named Sharpness Aware Minimization (SAM). Built on top of gradient based optimizers such as SGD or Adam (Kingma & Ba, 2015), SAM searches for a loss maximum in a limited parameter vicinity for each optimization step and calculates the loss gradient at this ascended parameter position. To construct a computationally feasible training algorithm, SAM approximates the loss landscape linearly so that the maximization is reduced to a single gradient ascent step. Moreover, this step is performed on a single batch rather than the full training set.

Unfortunately, the ascent step requires an additional forward and backward pass and therefore doubles the computational time, limiting the applications of SAM severely. Even though the linear approximation of the loss landscape poses a vast simplification and Foret et al. (2021) showed that searching for the maximum with multiple iterations of projected gradient ascent steps indeed yields higher maxima, these maxima, however, do not improve the generalization, suggesting that finding the actual maximum in the local vicinity is not pivotal. Instead, it appears to be sufficient to alter the parameters to find an elevated point and perform the gradient calculation from there. Following this reasoning, the ascent step can be understood as a temporary parameter perturbation,

revealing strong resemblance of the SAM algorithm to extragradient methods (Korpelevich, 1976) and Nesterov Accelerated Gradient (Nesterov, 1983; Sutskever et al., 2013) which both calculate gradients at perturbed positions and were also discussed previously in the context of sharpness and generalization (Lin et al., 2020a; Wen et al., 2018).

Commonly, measures to address generalization issues are applied between the data distribution and the full training dataset (Keskar et al., 2017; Li et al., 2018). Since the generalization error is caused by the limited sample size, further reducing the regarded sample size to single batches might impose additional deteriorating effects. Thus motivated, we reconsider the effect of momentum in batch-based gradient optimization algorithms as follows. The momentum vector not only represents a trace over iterations in the loss landscape and therefore accumulates the gradients at past parameter positions, but also builds an exponential moving average over gradients of successive batches. Hence, the resultant momentum vector can also be seen as an approximation of the gradient of the loss on a larger subset - in the limiting case on the full training dataset.

Building on these observations and the theoretical framework of SAM, which assumes using the entire dataset for sharpness estimations, we present Momentum-SAM (MSAM). MSAM aims to minimize the global sharpness without imposing additional forward and backward pass computations by using the momentum direction as an approximated, yet less stochastic, direction for sharpness computations. In summary, our contribution is as follows:

- We propose Momentum-SAM (MSAM), an algorithm to minimize training loss sharpness without computational overhead over base optimizers such as SGD or Adam.
- The simplicity of our algorithm and the reduced computational costs enable the usage of sharpness-aware minimization for a variety of different applications without severely compromising the generalization capabilities and performance improvements of SAM.
- We discuss similarities and differences between MSAM and Nesterov Accelerated Gradient (NAG) and reveal novel perspectives on SAM, MSAM, as well as on NAG.
- We validate MSAM on multiple image classification benchmarks and compare MSAM against related sharpness-aware approaches.

1.1 RELATED WORK

Correlations between loss sharpness, generalization, and overfitting were studied extensively (Hochreiter & Schmidhuber, 1994; Keskar et al., 2017; Lin et al., 2020b; Yao et al., 2018; Li et al., 2018; Liu et al., 2020; Damian et al., 2021), all linking flatter minima to better generalization, while Dinh et al. (2017) showed that sharp minima can generalize too. While the above-mentioned works focus on analysing loss sharpness, algorithms to explicitly target sharpness reduction were suggested by Zheng et al. (2021); Wu et al. (2020); Chaudhari et al. (2017) with SAM (Foret et al., 2021) being most prevalent.

SAM relies on computing gradients at parameters distinct from the current iterations position. This resembles extragradient methods (Korpelevich, 1976) like Optimistic Mirror Descent (OMD) (Juditsky et al., 2011) or Nesterov Accelerated Gradient (NAG) (Nesterov, 1983; Sutskever et al., 2013) which were also applied to Deep Learning, either based on perturbations by last iterations gradients (Daskalakis et al., 2018; Lin et al., 2020a) or random perturbations (Wen et al., 2018).

Adaptive-SAM (ASAM) (Kwon et al., 2021) accommodates SAM by scaling the perturbations relative to the weights norms to take scale invariance between layers into account, resulting in a significant performance improvement over SAM. Furthermore, Kim et al. (2022) refine ASAM by considering Fisher information geometry of the parameter space. Also seeking to improve SAM, GSAM (Zhuang et al., 2022) posit that minimizing the perturbed loss might not guarantee a flatter loss and suggest using a combination of the SAM gradient and the SGD gradients component orthogonal to the SAM gradient for the weight updates.

Unlike the aforementioned methods, several algorithms were proposed to reduce SAMs runtime, mostly sharing the idea of reducing the number of additional forward/backward passes, in contrast to our approach which relies on finding more efficient parameter perturbations. For example, Jiang et al. (2023) are evaluating in each iteration if a perturbation calculation is to be performed. LookSAM Liu et al. (2022) updates perturbations only each k -th iterations and applies perturbation components orthogonal to SGD gradients in iterations in between. Mi et al. (2022) are following an approach based on sparse matrix operations and ESAM (Du et al., 2022b) combines parameter sparsification with the idea to reduce the number of input samples for second forward/backward passes. Similarly,

Bahri et al. (2021) and Ni et al. (2022) calculate perturbations on micro-batches. Not explicitly targeted at efficiency optimization, Mueller & Hein (2022) show that only perturbing Batch Norm layers even further improves SAM. SAF and its memory efficient version MESA were proposed by Du et al. (2022a), focusing on storing past iterations weights to minimize sharpness on the digits output instead of the loss function. Perturbations in momentum direction after the momentum buffer update resulting in better performance but no speedup were proposed by Li & Giannakis (2023). Furthermore, several concepts were proposed to explain the success of SAM and related approaches (Andriushchenko & Flammarion, 2022; Möllenhoff & Khan, 2023).

2 METHOD

2.1 NOTATION

Given a finite training dataset $\mathcal{S} \subset \mathcal{X} \times \mathcal{Y}$ where \mathcal{X} is the set of possible inputs and \mathcal{Y} the set of possible targets drawn from a joint distribution \mathcal{D} , we study a model $f_{\mathbf{w}} : \mathcal{X} \rightarrow \mathcal{Y}$ parameterized by $\mathbf{w} \in \mathcal{W}$, an element-wise loss function $l : \mathcal{W} \times \mathcal{X} \times \mathcal{Y} \rightarrow \mathbb{R}$, the distribution loss $L_{\mathcal{D}}(\mathbf{w}) = \mathbb{E}_{(x,y) \sim \mathcal{D}}(l(\mathbf{w}, x, y))$ and the empirical (training) loss $L_{\mathcal{S}}(\mathbf{w}) = 1/|\mathcal{S}| \sum_{(x,y) \in \mathcal{S}} l(\mathbf{w}, x, y)$. If calculated on a single batch $\mathcal{B} \subset \mathcal{S}$ we denote the loss as $L_{\mathcal{B}}$. We denote the L2-norm by $\|\cdot\|$.

2.2 SHARPNESS AWARE MINIMIZATION (SAM)

For many datasets modern neural network architectures and empirical risk minimization algorithms like SGD or Adam (Kingma & Ba, 2015) effectively minimize the approximation and optimization error (i.e. finding low $L_{\mathcal{S}}(\mathbf{w})$), while reducing the generalization error ($L_{\mathcal{D}}(\mathbf{w}) - L_{\mathcal{S}}(\mathbf{w})$) remains a major challenge. Following ideas of Hochreiter & Schmidhuber (1994), Keskar et al. (2017) observed a link between sharpness of the minimized empirical loss $L_{\mathcal{S}}(\mathbf{w}^{\text{opt}})$ with respect to the parameters and the generalization error. Intuitively, this follows from the observation that perturbations in inputs (cf. adversarial training (Goodfellow et al., 2015)) and perturbations in parameters have a similar effect on network outputs (due to both being factors in matrix-vector products) and that the generalization error is caused by the limitation to a smaller input subset which resembles an input perturbation. Without giving an explicit implementation, Keskar et al. (2017) sketches the idea of avoiding sharp minima by replacing the empirical loss minimization with a minimization of the highest loss value within a ball in parameter space of fixed size ρ :

$$\min_{\mathbf{w}} \max_{\|\epsilon\| \leq \rho} L_{\mathcal{S}}(\mathbf{w} + \epsilon) \quad (1)$$

Foret et al. (2021) propose a computationally feasible algorithm to approximate this training objective via so-called Sharpness Aware Minimization (SAM). SAM heavily reduces the computational costs of the inner maximization routine of Eq. 1 by approximating the loss landscape in first order, neglecting second order derivatives resulting from the min-max objective, and performing the maximization on single batches (or per GPU in case of m -sharpness). These simplifications result in adding one gradient ascent step with fixed step length before the gradient calculation, i.e., reformulating the loss as

$$L_{\mathcal{B}}^{\text{SAM}}(\mathbf{w}) := L_{\mathcal{B}}(\mathbf{w} + \epsilon^{\text{SAM}}) \text{ where } \epsilon^{\text{SAM}} := \rho \frac{\nabla L_{\mathcal{B}}(\mathbf{w})}{\|\nabla L_{\mathcal{B}}(\mathbf{w})\|}. \quad (2)$$

The parameters are temporarily perturbed by ϵ^{SAM} in the direction of the locally highest slope with the perturbation removed again after gradient calculation. Thus, the parameters are not altered permanently. While performance improvements could be achieved (Foret et al., 2021; Chen et al., 2022) the computation of ϵ^{SAM} demands an additional backward pass and the computation of $L_{\mathcal{B}}(\mathbf{w} + \epsilon^{\text{SAM}})$ an additional forward pass, resulting in roughly doubling the runtime of SAM compared to base optimizer like SGD or Adam.

Minimizing Eq. 2 can also be interpreted as jointly minimizing the unperturbed loss function $L_{\mathcal{B}}(\mathbf{w})$ and the sharpness of the loss landscape defined by

$$S_{\mathcal{B}}(\mathbf{w}) := L_{\mathcal{B}}(\mathbf{w} + \epsilon) - L_{\mathcal{B}}(\mathbf{w}). \quad (3)$$

2.3 MOMENTUM AND NESTEROV ACCELERATED GRADIENT

Commonly, SGD is used with momentum, i.e., instead of updating parameters by gradients directly ($\mathbf{w}_{t+1} = \mathbf{w}_t - \eta \nabla L_{\mathcal{B}_t}(\mathbf{w}_t)$ with learning rate η), an exponential moving average of past

gradients is used for the updates. Given the momentum factor μ and the momentum vector $\mathbf{v}_{t+1} = \mu\mathbf{v}_t + \nabla L_{\mathcal{B}_t}(\mathbf{w}_t)$ the update rule becomes $\mathbf{w}_{t+1} = \mathbf{w}_t - \eta\mathbf{v}_{t+1}$.

The momentum vector has two averaging effects. First, it averages the gradient at different positions in the parameter space \mathbf{w}_t and second, it averages the gradient over multiple batches \mathcal{B}_t which can be interpreted as an increase of the effective batch size.

The update step consists of the momentum vector of the past iteration and the present iterations gradient. While this gradient is calculated prior to the momentum vector update in standard momentum training, NAG instead calculates the gradient after the momentum vector step is performed. The update rule for the momentum vector thus becomes $\mathbf{v}_{t+1} = \mu\mathbf{v}_t + \nabla L_{\mathcal{B}_t}(\mathbf{w}_t - \eta\mu\mathbf{v}_t)$. Analogously to Eq. 2, NAG can be formulated in terms of a perturbed loss function as

$$L_{\mathcal{B}}^{\text{NAG}}(\mathbf{w}) := L_{\mathcal{B}}(\mathbf{w} + \epsilon^{\text{NAG}}) \text{ where } \epsilon^{\text{NAG}} := -\eta\mu\mathbf{v}_t. \quad (4)$$

Since the perturbation vector ϵ^{NAG} neither depends on the networks output nor its gradient at step t no additional forward or backward pass is needed.

Algorithm 1: SGD with Momentum-SAM (MSAM; efficient implementation)

Input: training data \mathcal{S} , momentum μ , learning rate η , perturbation strength ρ

Initialize: weights $\tilde{\mathbf{w}}_0 \leftarrow$ random, momentum vector $\mathbf{v}_0 \leftarrow 0$

for $t \leftarrow 0$ **to** T **do**

 sample batch $\mathcal{B}_t \subset \mathcal{S}$

$L_{\mathcal{B}_t}(\tilde{\mathbf{w}}_t) = 1/|\mathcal{B}_t| \sum_{(x,y) \in \mathcal{B}_t} l(\tilde{\mathbf{w}}_t, x, y)$ // perturbed forward pass

$\mathbf{g}_{\text{MSAM}} = \nabla L_{\mathcal{B}_t}(\tilde{\mathbf{w}}_t)$ // perturbed backward pass

$\mathbf{w}_t = \tilde{\mathbf{w}}_t + \rho \frac{\mathbf{v}_t}{\|\mathbf{v}_t\|}$ // remove last perturbation

$\mathbf{v}_{t+1} = \mu\mathbf{v}_t + \mathbf{g}_{\text{MSAM}}$ // update momentum vector

$\mathbf{w}_{t+1} = \mathbf{w}_t - \eta\mathbf{v}_{t+1}$ // SGD step

$\tilde{\mathbf{w}}_{t+1} = \mathbf{w}_{t+1} - \rho \frac{\mathbf{v}_{t+1}}{\|\mathbf{v}_{t+1}\|}$ // perturb for next iteration

end

$\mathbf{w}_T = \tilde{\mathbf{w}}_T + \rho \frac{\mathbf{v}_T}{\|\mathbf{v}_T\|}$ // remove final perturbation

return \mathbf{w}_T

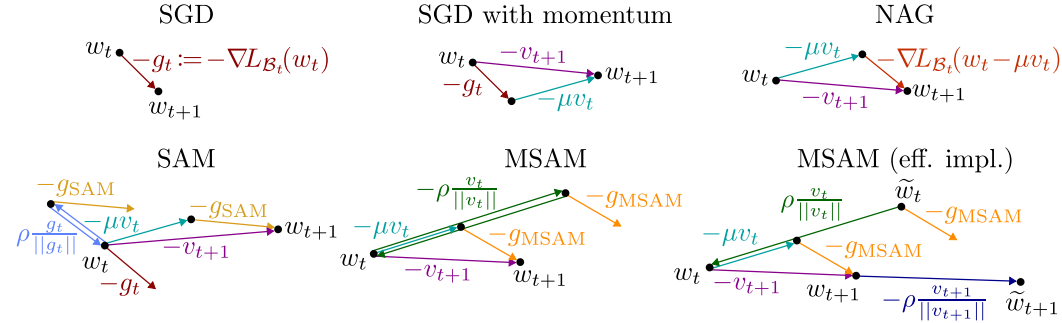


Figure 1: Schematic illustrations of optimization algorithms based on SGD. NAG calculates gradients after updating parameters with the momentum vector. SAM and MSAM calculate gradients at perturbed positions but remove perturbations again before the parameter update step. See Alg. 1 for detailed description of the efficient implementation of MSAM.

2.4 MOMENTUM-SAM

Foret et al. (2021) show that performing multiple iterations of projected gradient ascent in the inner maximization does result in parameters with higher loss inside the ρ -ball (cf. Eq. 1). However, and counterintuitively, this improved inner maximization does not yield a better generalization of the model. We conclude that finding the exact (per batch) local maximum is not pivotal to SAM. Inspired by NAG and given that the theoretical framework of sharpness minimization is based on calculating the sharpness on the full training dataset, we propose using the momentum vector as the perturbation direction and call the resulting algorithm Momentum-SAM (MSAM) (further perturbations are

discussed in Appx. A.7). Following the above notation, this yields the loss objective

$$L_{\mathcal{B}}^{\text{MSAM}}(\mathbf{w}) := L_{\mathcal{B}}(\mathbf{w} + \epsilon^{\text{MSAM}}) \text{ where } \epsilon^{\text{MSAM}} := -\rho \frac{\mathbf{v}_t}{\|\mathbf{v}_t\|}. \quad (5)$$

Contrary to SAM, we perturb in the negative direction. Since we use the momentum vector before it is updated, a step in the negative direction of the momentum has already been performed in the iteration before, thus, the loss is expected to increase again for sufficiently large step sizes. The stepsize by ϵ^{MSAM} is typically at least one order of magnitude higher than learning rate steps, so we overshoot local minima in momentum direction and reach an increased perturbed loss offering a suitable direction for sharpness estimation. We empirically show that the momentum descent step actually results in an ascent on the per-batch loss in Sec. 4.1 and Sec. A.11. For an efficient implementation, we shift the starting point of each iteration to be the perturbed parameters $\tilde{\mathbf{w}}_t = \mathbf{w}_t - \rho \mathbf{v}_t / \|\mathbf{v}_t\|$ (in analogy to common implementations of NAG) and remove the final perturbation after the last iteration (see Alg. 1). All mentioned optimization strategies are depicted in detail in Fig. 1. Since SGD with momentum as well as Adam store a running mean of gradients, MSAM does not take up additional memory and comes with negligible computational overhead.

Furthermore, we confirm that a similar theoretical generalization bound as reported by Foret et al. (2021) also holds for directions of high curvature as the momentum direction (see Appx. A.1).

3 EXPERIMENTAL RESULTS

3.1 SPEED AND ACCURACY FOR RESNETS ON CIFAR100

Table 1: Comparison against multiple (sharpness-aware) optimizers. Baseline optimizers are SGD for CIFAR100 and AdamW for ImageNet. Please see Appx. A.5 for experimental details. MSAM outperforms optimizers of equal speed (AdamW/SGD and NAG) and alternative approaches for faster sharpness reduction.

Optimizer	CIFAR100			ImageNet	Speed
	WRN-28-10	WRN-16-4	ResNet-50	ViT-S/32	
SAM	84.16±0.12	79.25±0.10	83.36±0.17	69.1	0.52
Baseline	81.51±0.09	76.90±0.15	81.46±0.13	67.0	1.00
NAG	82.00±0.11	77.09±0.18	82.12±0.12	—	0.99
LookSAM	83.31 ±0.12	79.00 ±0.08	82.24±0.11	68.0	0.84
ESAM	82.71±0.38	77.79±0.11	80.49±0.40	66.1	0.62
MESA	82.75±0.08	78.32±0.08	81.94±0.26	69.0	0.77
MSAM (ours)	83.21 ±0.07	79.11 ±0.09	82.65 ±0.12	69.1	0.99

In Tab. 1, we show test accuracies for MSAM and related optimizers for WideResNet-28-10, WideResNet-16-4 (Zagoruyko & Komodakis, 2016) and ResNet50 (He et al., 2016) on CIFAR100 (Krizhevsky & Hinton, 2009) and ImageNet-1k (Deng et al., 2009) next to the training speed. We first tuned the learning rate and weight decay for SGD/AdamW and then optimized ρ for each model (see Appx. A.4 for more details). Additionally, we conducted experiments with related approaches which seek to make SAM more efficient, namely ESAM (Du et al., 2022b), LookSAM (Liu et al., 2022) and MESA (Du et al., 2022a). While Du et al. (2022a) also proposed a second optimizer (SAF), we decided to compare against the memory-efficient version MESA (as recommended by the authors for e.g. ImageNet). Note that LookSAM required tuning of an additional hyperparameter. See Appx. A.5 for implementation details on the related optimizers. Optimizers of the same speed as MSAM (i.e. SGD/AdamW and NAG) are significantly outperformed. While SAM reaches slightly higher accuracies than MSAM, twice as much runtime is needed. Accuracies of MSAM and LookSAM do not differ significantly for WideResNets, however, MSAM performs better on ResNet-50, is faster, and does not demand additional hyperparameter tuning. For ESAM we observed only a minor speedup compared to SAM and the accuracies of MSAM could not be reached. MESA yields similar results to MSAM for ViT on ImageNet but performs worse on all models on CIFAR100 and is slower compared to MSAM.

3.2 RESNET AND ViT ON IMAGENET RESULTS

Moreover, we test MSAM for ResNets (He et al., 2016) and further ViT variants (Dosovitskiy et al., 2021) on ImageNet-1k (Deng et al., 2009) and report results in Tab. 2. Due to limited computational resources, we only run single iterations, but provide an estimate of the uncertainty by running 5 iterations of baseline optimizers for the smallest models per category and calculate the standard deviations. During the learning rate warm-up phase commonly used for ViTs we set $\rho_{\text{MSAM}} = 0$. SAM also benefits from this effect, but less pronounced, so we kept SAM active during warm-up phase to stay consistent with related work (see Appx. A.3 for detailed discussion). While performance improvements are small for ResNets for MSAM and SAM, both optimizers achieve clear improvements for ViTs. Even though slightly below SAMs performance for most models, MSAM yields comparable results while being almost twice as fast.

In addition, we conducted experiments for ViT-S/32 on ImageNet when giving MSAM the same computational budget as SAM (i.e. training for 180 epochs) yielding a test accuracy of 70.1% and thus clearly outperforming SAMs 69.1% (also see Appx. A.9).

Table 2: Test accuracies on ImageNet for baseline optimizers (SGD or AdamW), SAM and MSAM. Estimated uncertainties: ResNet: ± 0.08 , ViT (90 epochs): ± 0.17 , ViT (300 epochs): ± 0.24 . Improvements over baseline are given in green. MSAM yields results comparable to SAM for most models while being ≈ 2 times faster in all our experiments.

Model	Epochs	Baseline		SAM	MSAM
ResNet-50	100	SGD	76.3	76.6 ^{+0.3}	76.5 ^{+0.2}
ResNet-101	100	SGD	77.9	78.7 ^{+0.8}	78.2 ^{+0.3}
ViT-S/32	300	AdamW	67.2	71.4 ^{+4.2}	70.5 ^{+3.3}
	90	AdamW	67.0	69.1 ^{+2.1}	69.1 ^{+2.1}
ViT-S/16	300	AdamW	73.0	78.2 ^{+5.2}	75.8 ^{+2.8}
	90	AdamW	72.6	75.8 ^{+3.2}	74.9 ^{+2.3}
ViT-B/32	90	AdamW	66.9	70.4 ^{+3.5}	70.2 ^{+3.3}
ViT-B/16	90	AdamW	73.0	77.7 ^{+4.7}	75.7 ^{+2.7}

3.3 COMBINATION WITH OTHER SAM VARIANTS

As shown by Kwon et al. (2021), weighting the perturbation components by the parameters significantly improves SAM. Similarly, Mueller & Hein (2022) showed that applying the perturbations only to the Batch Norm layers (Ioffe & Szegedy, 2015) yields further enhancements. Both of these techniques can also be applied to MSAM, yielding test results similar to SAM (see Tab. 3).

Table 3: Test accuracy for different variants of MSAM/SAM on CIFAR100. Adaptive refers to ASAM (Kwon et al., 2021) and BN-only to applying the perturbation only to Batch Norm layers (cf. Mueller & Hein (2022)). MSAM performs well with both variants.

Optimizer		WRN-28-10	WRN-16-4	ResNet-50
SGD		81.51 \pm 0.09	76.90 \pm 0.15	81.46 \pm 0.13
vanilla	SAM	84.16 \pm 0.12	79.25 \pm 0.10	83.36 \pm 0.17
	MSAM	83.21 \pm 0.07	79.11 \pm 0.09	82.65 \pm 0.12
adaptive	SAM	84.74 \pm 0.13	79.96 \pm 0.13	83.30 \pm 0.06
	MSAM	84.15 \pm 0.13	79.89 \pm 0.09	83.48 \pm 0.08
BN-only	SAM	84.57 \pm 0.07	79.73 \pm 0.24	84.51 \pm 0.17
	MSAM	83.62 \pm 0.09	79.73 \pm 0.14	83.49 \pm 0.19

4 PROPERTIES OF MSAM

4.1 OPTIMIZATION AND GENERALIZATION ANALYSIS

Instead of ascending along the positive gradient as in SAM, we propose perturbing along the negative momentum vector (positive ρ^{MSAM} in our notation) as it is also done by extragradient methods like Lin et al. (2020a). We did not observe any increase in test performance when perturbing in the positive momentum direction (negative ρ^{MSAM}). In fact, negative ρ values cause a rapid decrease in test accuracy, whereas positive ρ values cause a gain in test accuracy of more than 2% for a WideResNet-16-4 trained on CIFAR100 as depicted in Fig. 2A, while NAG only provides minor improvements.

Fig. 2B shows the same data on logarithmic scale next to the test accuracy. The ordinate limits are chosen such that baseline (SGD) accuracies as well as maximal gains by MSAM align. NAG improves the training accuracy greatly, especially compared to the gains in test accuracy. This underlines that NAG is designed to foster the optimization procedure (ERM) but does not improve the generalization capabilities of the model. Similarly, for MSAM the maximal test accuracy is reached for high values of ρ where the train accuracy dropped far below the baseline, emphasising the effect of MSAM on the generalization instead of optimization.

Furthermore, small negative values of ρ induce a steep decrease in training accuracy while the test accuracy is not significantly affected, but drops for higher negative ρ . This might offer an explanation why MSAM does not improve the test accuracy with negative ρ values. A perturbation in the positive momentum vector direction resembles a step back to past iterations which might result in the gradient not encoding appropriate present or future information about the optimization direction and thus seems to be ill-suited to reduce the training loss effectively, counteracting the benefits of the increased generalization (larger test-train gap). SAM might not suffer from this effect, since the local (per batch) gradient does not encode much of the general optimization direction (which is dominated by the momentum vector), hence, the perturbed parameters disagree with parameters from previous iterations.

Counterintuitively, the cosine similarity between the momentum vector v_{t-1} and the gradient $g_t = \nabla L_{B_t}(w_t)$ is negative for most iterations (though nears zero at the end of training; see Fig. 2C). Thus, the negative momentum direction actually has a positive slope, so that perturbing in this direction resembles an ascent on the per-batch loss, further supporting the analogy of MSAM and SAM, and offering an explanation for the benefit of the negative sign (see Appx. A.11 for an empirical validation). Since an update step in the momentum direction was already performed, further moving in this direction overshoots the local minima and thus causes the positive slope. This is also in line with our theoretical considerations in Appx. A.1. Independently of sharpness minimization, this observation might offer interesting insights to SGD in general and we intend to follow this up in future work.

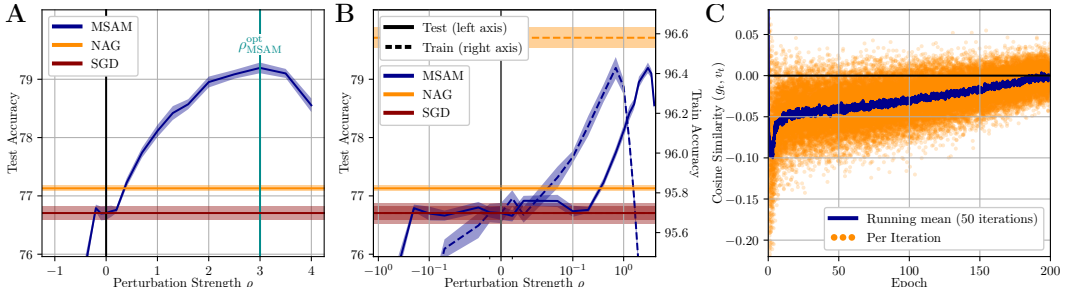


Figure 2: WideResNet-16-4 on CIFAR100 **A:** Test accuracy for positive and negative ρ compared against SGD and NAG. **B:** Train and test accuracy on logarithmic scale. **C:** Cosine similarity between momentum vector v_{t-1} and gradient $g_t = \nabla L_{B_t}(w_t)$. Momentum vector direction has mostly negative slope during training and approaches zero at the end.

4.2 SIMILARITY BETWEEN SAM AND MSAM

To support our hypotheses that MSAM yields a valid alternative to SAM, we investigate the similarity between the resulting gradients. After searching for the optimal value, we keep $\rho_{\text{SAM}} = 0.3$ fixed, train a model with SAM, and calculate the gradients

$$\mathbf{g}_{\text{SGD}} = \nabla L_{\mathcal{B}_t}(\mathbf{w}_t) \quad (6)$$

$$\mathbf{g}_{\text{SAM}} = \nabla L_{\mathcal{B}_t}(\mathbf{w}_t + \rho_{\text{SAM}} \nabla L_{\mathcal{B}_t}(\mathbf{w}_t)) / \|\nabla L_{\mathcal{B}_t}(\mathbf{w}_t)\| \quad (7)$$

$$\mathbf{g}_{\text{MSAM}}(\rho_{\text{MSAM}}) = \nabla L_{\mathcal{B}_t}(\mathbf{w}_t - \rho_{\text{MSAM}} \mathbf{v}_t / \|\mathbf{v}_t\|) \quad (8)$$

while we keep ρ_{MSAM} as a free parameter. To eliminate gradient directions which do not contribute in distinguishing between SAM and SGD gradients, we first project \mathbf{g}_{MSAM} into the plane spanned by \mathbf{g}_{SAM} and \mathbf{g}_{SGD} and then calculate the angle θ to \mathbf{g}_{SAM} (see Fig. 3A). By repeating this every 50 iterations for various values ρ_{MSAM} and calculating the value of zero-crossing ρ_0 , we determine when the maximal resemblance to SAM is reached (see Fig. 3B). As shown in Fig. 3C, ρ_0 reaches values close to the optimal regime of $\rho_{\text{MSAM}}^{\text{opt}} \approx 3$ (cf. Fig. 2A) for most epochs. While this correlation does not yield strict evidence it offers additional empirical support for the similarity between SAM and MSAM gradients.

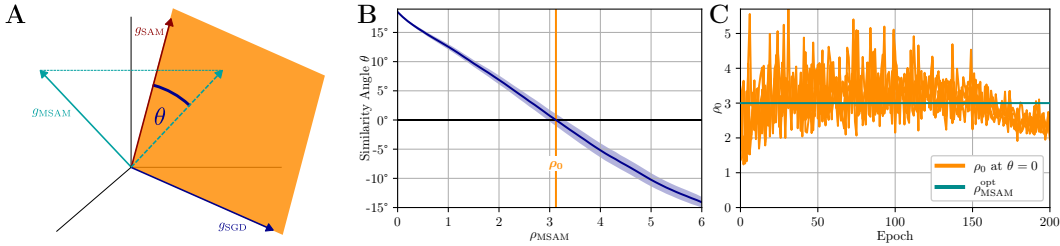


Figure 3: **A:** Projecting \mathbf{g}_{MSAM} into the plane of \mathbf{g}_{SAM} and \mathbf{g}_{SGD} to measure SAM/MSAM similarity. **B:** Varying ρ_{MSAM} until maximal similarity is reached (i.e. $\theta = 0$) and determine ρ_0 . **C:** ρ_{MSAM} at maximal similarity ρ_0 is close to generalization optimality ($\rho_{\text{MSAM}}^{\text{opt}}$, cf. Fig. 2A) for most epochs.

4.3 LOSS SHARPNESS ANALYSIS

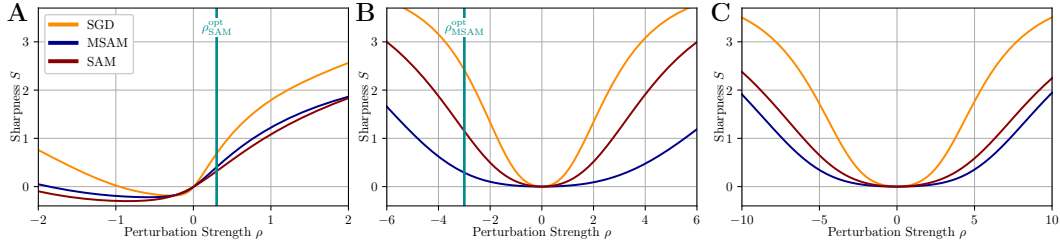


Figure 4: Sharpness (Eq. 3) after full training (200 epochs) for WideResNet-16-4 on CIFAR100 along different directions ϵ scaled by ρ . **A:** Gradient direction (as used as perturbation in SAM). **B:** Momentum direction (as in MSAM). **C:** Random filter-normalized direction as in Li et al. (2018). Vertical line at ρ^{opt} marks values of optimal test performance (cf. Fig. A.3A). MSAM and SAM are reducing their respective optimization objective best while MSAM reaches the lowest sharpness along random directions.

As mentioned above (and discussed by Foret et al. (2021)), the SAM implementation performs the loss maximization step on a single data batch instead of the full training set ($L_{\mathcal{B}}$ vs. $L_{\mathcal{S}}$). To analyze the efficacy of SAMs sharpness minimization, we therefore compare the sharpness (cf. Eq. 3) in the direction of local (per batch) gradients for models after full training with SGD, SAM and MSAM as a function of the perturbation scale ρ in Fig. 4A. The minima in local gradient directions are shifted from $\rho = 0$, since parameters found after training are usually not minima but saddle points (Dauphin et al., 2014). Compared to the other optimizers, SAM successfully minimizes the sharpness,

especially at optimal ρ_{opt} (as used during training).

The sharpness in momentum direction (Fig. 4B) represents the MSAM objective (Eq. 5). Here we do not include the negative sign in the definition of ϵ (as in Eq. 5), hence ρ_{opt} is negative. As expected, MSAM reduces this sharpness best. In contrast to the definition before, the sharpness is symmetric now for positive and negative signs. While MSAM only minimizes the sharpness in the negative direction explicitly, the positive direction is reduced jointly, further supporting the validity of perturbations in the negative momentum direction.

In Fig. 4C, we choose filter-normalized random vectors as perturbations as in Li et al. (2018). Since the loss landscape is rotational symmetric around the origin for multiple directions (as used in the original paper), we confine our analysis to one perturbation dimension. MSAM reaches the lowest sharpness, while both MSAM and SAM, significantly flatten the loss. This might be caused by MSAM approximating the maximization of L_S better due to the momentum vector v_t being an aggregation of gradients of multiple batches.

Interestingly, this relates to the findings of Foret et al. (2021) regarding m -sharpness, where the authors performed the maximization on even smaller data samples (fractions of batches per GPU in distributed training), yielding even better generalization. In this sense MSAM, reduces m even further over ordinary SAM ($m = 1$). In the same line of argument and despite being more efficient, MSAM oftentimes does not improve generalization compared to SAM. However, contradicting the general idea behind correlations of generalization and sharpness, MSAM yields flatter minima (if defined as in Fig. 4C), hence, indicating that explanations for the improved generalization of SAM/MSAM go beyond the reduction in sharpness.

We additionally analyze the loss curvature for SGD, SAM and MSAM in Appx. A.2.

4.4 NORMALIZATION

To gain a better understanding of the relation between MSAM and NAG, we conducted an ablation study by gradually altering the MSAM algorithm until it matches NAG. Firstly, we drop the normalization of the perturbation ϵ (numerator in Eq. 5), then we reintroduce the learning rate η to scale ϵ , and finally set $\rho = 1$ to arrive at NAG. Train and test accuracies as functions of ρ are shown in Fig. 5 for all variants. Dropping the normalization only causes a shift of ρ indicating that changes of the momentum norm during training are negligible. However, scaling by η drastically impacts the performance. Since the model is trained with a cosine learning rate scheduler (Loshchilov & Hutter, 2017), ρ decays jointly with η . The train accuracy is increased significantly not only for $\rho = 1$ (NAG), but even further for higher ρ , while the test performance drops at the same time when compared to MSAM. Thus, optimization is improved again while generalization is not, revealing separable mechanisms for test performance improvements of MSAM and NAG. High disturbances compared to the step size at the end of training appear to be crucial for increased generalization. Extensively investigating the effect of SAM/MSAM during different stages of training might offer potential to make SAM even more effective and/or efficient (i.e. by scheduling ρ to only apply disturbances for selected episodes).

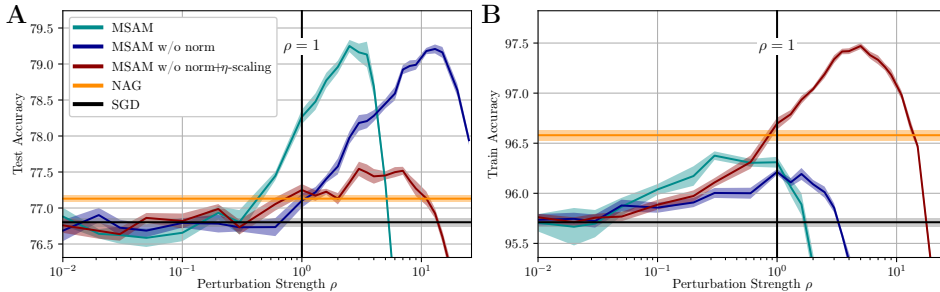


Figure 5: Test (A) and train (B) accuracy for WideResNet-16-4 on CIFAR100 for different normalization schemes of MSAM in dependence on ρ . MSAM without normalization works equally well. If the perturbation ϵ is scaled by learning rate η train performance (optimization) is increased while test performance (generalization) benefits only marginally.

5 CONCLUSION

In this work we introduced Momentum-SAM (MSAM), an optimizer achieving comparable results to the SAM optimizer while requiring no significant computational or memory overhead over optimizers such as Adam or SGD, hence, halving the computational load compared to SAM. On the one hand, this reduces the major hindrance for a widespread application of SAM-like algorithms when training resources are limited. On the other hand, we showed that perturbations independent of local gradients (in particular the momentum direction) can yield significant performance enhancements. Given the affinity of MSAM and NAG, we demonstrated new perspectives on SAM/MSAM as well as on NAG and underlined the importance as well as the need for future research of scaling and scheduling of perturbations to further improve sharpness-aware optimizers.

ACKNOWLEDGEMENTS

This work was funded by the Deutsche Forschungsgemeinschaft (DFG CRC 1459; Project-ID 433682494).

REFERENCES

- Maksym Andriushchenko and Nicolas Flammarion. Towards understanding sharpness-aware minimization. In *International Conference on Machine Learning*, pp. 639–668, 2022.
- Dara Bahri, Hossein Mobahi, and Yi Tay. Sharpness-aware minimization improves language model generalization. In *Annual Meeting of the Association for Computational Linguistics*, 2021.
- Lucas Beyer, Xiaohua Zhai, and Alexander Kolesnikov. Better plain vit baselines for imagenet-1k. *CoRR*, abs/2205.01580, 2022.
- Ondrej Bojar, Rajen Chatterjee, Christian Federmann, Yvette Graham, Barry Haddow, Matthias Huck, Antonio Jimeno Yepes, Philipp Koehn, Varvara Logacheva, Christof Monz, Matteo Negri, Aurelie Neveol, Mariana Neves, Martin Popel, Matt Post, Raphael Rubino, Carolina Scarton, Lucia Specia, Marco Turchi, Karin Verspoor, and Marcos Zampieri. Findings of the 2016 conference on machine translation. In *Proceedings of the First Conference on Machine Translation*, pp. 131–198, Berlin, Germany, August 2016. Association for Computational Linguistics.
- Pratik Chaudhari, Anna Choromanska, Stefano Soatto, Yann LeCun, Carlo Baldassi, Christian Borgs, Jennifer Chayes, Levent Sagun, and Riccardo Zecchina. Entropy-SGD: Biasing gradient descent into wide valleys. In *International Conference on Learning Representations*, 2017.
- Xiangning Chen, Cho-Jui Hsieh, and Boqing Gong. When vision transformers outperform resnets without pre-training or strong data augmentations. In *International Conference on Learning Representations*, 2022.
- Alex Damian, Tengyu Ma, and Jason D. Lee. Label noise SGD provably prefers flat global minimizers. In *Advances in Neural Information Processing Systems*, pp. 27449–27461, 2021.
- Constantinos Daskalakis, Andrew Ilyas, Vasilis Syrgkanis, and Haoyang Zeng. Training gans with optimism. In *International Conference on Learning Representations*, 2018.
- Yann N. Dauphin, Razvan Pascanu, Çağlar Gülçehre, KyungHyun Cho, Surya Ganguli, and Yoshua Bengio. Identifying and attacking the saddle point problem in high-dimensional non-convex optimization. In *Advances in Neural Information Processing Systems*, pp. 2933–2941, 2014.
- Jia Deng, Wei Dong, Richard Socher, Li-Jia Li, Kai Li, and Li Fei-Fei. Imagenet: A large-scale hierarchical image database. In *Proceedings of the IEEE/CVF Conference on Computer Vision and Pattern Recognition (CVPR)*, pp. 248–255, 2009.
- Laurent Dinh, Razvan Pascanu, Samy Bengio, and Yoshua Bengio. Sharp minima can generalize for deep nets. In *Proceedings of the 34th International Conference on Machine Learning*, pp. 1019–1028, 2017.
- Alexey Dosovitskiy, Lucas Beyer, Alexander Kolesnikov, Dirk Weissenborn, Xiaohua Zhai, Thomas Unterthiner, Mostafa Dehghani, Matthias Minderer, Georg Heigold, Sylvain Gelly, Jakob Uszkoreit, and Neil Houlsby. An image is worth 16x16 words: Transformers for image recognition at scale. In *International Conference on Learning Representations*, 2021.
- Jiawei Du, Zhou Daquan, Jiashi Feng, Vincent Tan, and Joey Tianyi Zhou. Sharpness-aware training for free. In *Advances in Neural Information Processing Systems*, 2022a.
- Jiawei Du, Hanshu Yan, Jiashi Feng, Joey Tianyi Zhou, Liangli Zhen, Rick Siow Mong Goh, and Vincent Tan. Efficient sharpness-aware minimization for improved training of neural networks. In *International Conference on Learning Representations*, 2022b.

-
- Pierre Foret, Ariel Kleiner, Hossein Mobahi, and Behnam Neyshabur. Sharpness-aware minimization for efficiently improving generalization. In *International Conference on Learning Representations*, 2021.
- Ian J. Goodfellow, Jonathon Shlens, and Christian Szegedy. Explaining and harnessing adversarial examples. In *International Conference on Learning Representations*, 2015.
- Kaiming He, Xiangyu Zhang, Shaoqing Ren, and Jian Sun. Deep residual learning for image recognition. In *Proceedings of the IEEE/CVF Conference on Computer Vision and Pattern Recognition (CVPR)*, pp. 770–778, 2016.
- Sepp Hochreiter and Jürgen Schmidhuber. Simplifying neural nets by discovering flat minima. In *Advances in Neural Information Processing Systems*, 1994.
- Sergey Ioffe and Christian Szegedy. Batch normalization: Accelerating deep network training by reducing internal covariate shift. In Francis R. Bach and David M. Blei (eds.), *Proceedings of the 32nd International Conference on Machine Learning*, pp. 448–456, 2015.
- Weisen Jiang, Hansi Yang, Yu Zhang, and James Kwok. An adaptive policy to employ sharpness-aware minimization. In *International Conference on Learning Representations*, 2023.
- Anatoli Juditsky, Arkadi Nemirovski, and Claire Tauvel. Solving variational inequalities with stochastic mirror-prox algorithm. *Stochastic Systems*, 1(1):17–58, 2011.
- Nitish Shirish Keskar, Dheevatsa Mudigere, Jorge Nocedal, Mikhail Smelyanskiy, and Ping Tak Peter Tang. On large-batch training for deep learning: Generalization gap and sharp minima. In *International Conference on Learning Representations*, 2017.
- Minyoung Kim, Da Li, Shell X Hu, and Timothy Hospedales. Fisher SAM: Information geometry and sharpness aware minimisation. In *Proceedings of the 39th International Conference on Machine Learning*, pp. 11148–11161, 2022.
- Diederik P. Kingma and Jimmy Ba. Adam: A method for stochastic optimization. In *International Conference on Learning Representations*, 2015.
- G. M. Korpelevich. The extragradient method for finding saddle points and other problems. In *Ekonomika i Matematicheskie Metody*, volume 12, pp. 747–756, 1976.
- Alex Krizhevsky and Geoffrey Hinton. Learning multiple layers of features from tiny images. Technical report, University of Toronto, Toronto, Ontario, 2009.
- Jungmin Kwon, Jeongseop Kim, Hyunseo Park, and In Kwon Choi. Asam: Adaptive sharpness-aware minimization for scale-invariant learning of deep neural networks. In *Proceedings of the 38th International Conference on Machine Learning*, pp. 5905–5914, 2021.
- Bingcong Li and Georgios B. Giannakis. Enhancing sharpness-aware optimization through variance suppression. In *Thirty-seventh Conference on Neural Information Processing Systems*, 2023. URL <https://openreview.net/forum?id=Sf3t6Bth4P>.
- Hao Li, Zheng Xu, Gavin Taylor, Christoph Studer, and Tom Goldstein. Visualizing the loss landscape of neural nets. In *Advances in Neural Information Processing Systems*, 2018.
- Tao Lin, Lingjing Kong, Sebastian Stich, and Martin Jaggi. Extrapolation for large-batch training in deep learning. In *Proceedings of the 37th International Conference on Machine Learning*, pp. 6094–6104, 2020a.
- Tao Lin, Sebastian U. Stich, Kumar Kshitij Patel, and Martin Jaggi. Don’t use large mini-batches, use local SGD. In *International Conference on Learning Representations*, 2020b.
- Chen Liu, Mathieu Salzmann, Tao Lin, Ryota Tomioka, and Sabine Süsstrunk. On the loss landscape of adversarial training: Identifying challenges and how to overcome them. In *Advances in Neural Information Processing Systems*, 2020.

-
- Yong Liu, Siqi Mai, Xiangning Chen, Cho-Jui Hsieh, and Yang You. Towards efficient and scalable sharpness-aware minimization. In *Proceedings of the IEEE/CVF Conference on Computer Vision and Pattern Recognition*, pp. 12360–12370, 2022.
- Ilya Loshchilov and Frank Hutter. SGDR: stochastic gradient descent with warm restarts. In *International Conference on Learning Representations*, 2017.
- Peng Mi, Li Shen, Tianhe Ren, Yiyi Zhou, Xiaoshuai Sun, Rongrong Ji, and Dacheng Tao. Make sharpness-aware minimization stronger: A sparsified perturbation approach. In *Advances in Neural Information Processing Systems*, 2022.
- Thomas Möllenhoff and Mohammad Emtiyaz Khan. SAM as an optimal relaxation of bayes. In *International Conference on Learning Representations*, 2023.
- Maximilian Mueller and Matthias Hein. Perturbing batchnorm and only batchnorm benefits sharpness-aware minimization. In *Has it Trained Yet? NeurIPS 2022 Workshop*, 2022.
- Preetum Nakkiran, Gal Kaplun, Yamini Bansal, Tristan Yang, Boaz Barak, and Ilya Sutskever. Deep double descent: Where bigger models and more data hurt. *Journal of Statistical Mechanics: Theory and Experiment*, 2021(12):124003, 2021.
- Y. Nesterov. A method for solving a convex programming problem with convergence rate $o(1/k^2)$, 1983.
- Renkun Ni, Ping yeh Chiang, Jonas Geiping, Micah Goldblum, Andrew Gordon Wilson, and Tom Goldstein. K-sam: Sharpness-aware minimization at the speed of sgd, 2022.
- Colin Raffel, Noam Shazeer, Adam Roberts, Katherine Lee, Sharan Narang, Michael Matena, Yanqi Zhou, Wei Li, and Peter J. Liu. Exploring the limits of transfer learning with a unified text-to-text transformer. *arXiv e-prints*, 2019.
- Ilya Sutskever, James Martens, George Dahl, and Geoffrey Hinton. On the importance of initialization and momentum in deep learning. In *Proceedings of the 30th International Conference on Machine Learning*, Proceedings of Machine Learning Research, pp. 1139–1147, 2013.
- Christian Szegedy, Wei Liu, Yangqing Jia, Pierre Sermanet, Scott E. Reed, Dragomir Anguelov, Dumitru Erhan, Vincent Vanhoucke, and Andrew Rabinovich. Going deeper with convolutions. In *Proceedings of the IEEE/CVF Conference on Computer Vision and Pattern Recognition (CVPR)*, pp. 1–9, 2015.
- Yi Tay, Mostafa Dehghani, Jinfeng Rao, William Fedus, Samira Abnar, Hyung Won Chung, Sharan Narang, Dani Yogatama, Ashish Vaswani, and Donald Metzler. Scale efficiently: Insights from pretraining and finetuning transformers. In *International Conference on Learning Representations*, 2022.
- Wei Wen, Yandan Wang, Feng Yan, Cong Xu, Yiran Chen, and Hai Li. Smoothout: Smoothing out sharp minima for generalization in large-batch deep learning. *CoRR*, abs/1805.07898, 2018.
- Dongxian Wu, Shu-Tao Xia, and Yisen Wang. Adversarial weight perturbation helps robust generalization. In *Advances in Neural Information Processing Systems*, pp. 2958–2969, 2020.
- Zhewei Yao, Amir Gholami, Qi Lei, Kurt Keutzer, and Michael W. Mahoney. Hessian-based analysis of large batch training and robustness to adversaries. In *Advances in Neural Information Processing Systems*, pp. 4954–4964, 2018.
- Sergey Zagoruyko and Nikos Komodakis. Wide residual networks. In *Proceedings of the British Machine Vision Conference*, 2016.
- Yaowei Zheng, Richong Zhang, and Yongyi Mao. Regularizing neural networks via adversarial model perturbation. In *Proceedings of the IEEE/CVF Conference on Computer Vision and Pattern Recognition (CVPR)*, pp. 8156–8165, 2021.
- Juntang Zhuang, Boqing Gong, Liangzhe Yuan, Yin Cui, Hartwig Adam, Nicha C Dvornek, sekhar tatikonda, James s Duncan, and Ting Liu. Surrogate gap minimization improves sharpness-aware training. In *International Eleventh Conference on Learning Representations*, 2022.

APPENDIX

A.1 THEORETICAL ANALYSIS OF MSAM

We build our analysis in analogy to Foret et al. (2021). While Foret et al. (2021) proofed the existence of an upper generalization bound if the parameters with the highest loss in a fixed ρ -ball are found, we show that a similar bound can also be derived by simply assuming perturbations in directions of high curvature. In practice this first assumption is fulfilled by the momentum vector \mathbf{v}_t , since gradients are directions of high curvature. Secondly, if a properly tuned learning rate is used, the slope in momentum direction after the parameter update is either close to zero or even negative caused by overshooting marginally.

We state these two assumptions in Setting 1. While we empirically validate the first assumption in Appx. A.2, we already showed and discussed evidence for the second assumption in the main text (cf. Fig. 2C).

Proposition 1 *Let $\epsilon, \mathbf{v} \in \mathcal{W}$ with i.i.d. components $\epsilon_i \sim \mathcal{N}(0, \sigma)$ for some $\sigma > 0$, then for any $\rho > 0$*

$$\mathbb{E}[\mathbf{1}_{\{\|\epsilon\|_2 \leq \rho\}} \epsilon^T \text{Hess}(L_S(\mathbf{w})) \epsilon] \leq \rho^2 \kappa, \quad (9)$$

where $\kappa := \frac{1}{|\mathcal{W}|} \text{tr}[\text{Hess}(L_S(\mathbf{w}))]$.

Proof *W.L.O.G. we assume $\text{Hess}(L_S(\mathbf{w}))$ to be diagonal. The claim then follows from the linearity of the expectation and symmetry.* \square

Setting 1 *Let $\mathbf{w}, \mathbf{v} \in \mathcal{W}$ with $\|\mathbf{v}\|_2 = 1$ such that:*

- $\mathbf{v}^T \text{Hess}(L_S(\mathbf{w})) \mathbf{v} > \kappa$,
- $\nabla L_S(\mathbf{w}) \cdot \mathbf{v} \leq 0$.

Lemma 2 *Assume Setting 1 and let $\epsilon \in \mathcal{W}$ with $\epsilon_i \sim \mathcal{N}(0, \sigma)$, then it holds for any $\rho > 0$ that*

$$\mathbb{E}[\mathbf{1}_{\{\|\epsilon\|_2 \leq \rho\}} L_S(\mathbf{w} + \epsilon)] \leq L_S(\mathbf{w} - \rho \mathbf{v}) + \mathcal{O}(\rho^3).$$

Proof *Applying a Taylor expansion around \mathbf{w} yields:*

$$\begin{aligned} & \mathbb{E}[\mathbf{1}_{\{\|\epsilon\|_2 \leq \rho\}} L_S(\mathbf{w} + \epsilon)] \leq L_S(\mathbf{w} - \rho \mathbf{v}) \\ \iff & \underbrace{\mathbb{E}[\mathbf{1}_{\{\|\epsilon\|_2 \leq \rho\}} \nabla L_S(\mathbf{w}) \cdot \epsilon]}_{=0} + \underbrace{\mathbb{E}[\mathbf{1}_{\{\|\epsilon\|_2 \leq \rho\}} \epsilon^T \text{Hess}(L_S(\mathbf{w})) \epsilon]}_{\leq \rho^2 \kappa} \leq \\ & \underbrace{-\rho \nabla L_S(\mathbf{w}) \cdot \mathbf{v} + \rho^2 \mathbf{v}^T \text{Hess}(L_S(\mathbf{w})) \mathbf{v}}_{\geq 0} + \mathcal{O}(\rho^3) \\ & \iff \kappa \leq \mathbf{v}^T \text{Hess}(L_S(\mathbf{w})) \mathbf{v} + \mathcal{O}(\rho^3) \end{aligned}$$

subtracting the $\mathcal{O}(\rho^3)$ -term from the initial inequality then yields the claim. \square

Theorem 3 *Assume Setting 1 then for any distribution \mathfrak{D} , with probability $1 - \delta$ over the choice of the training Set $\mathcal{S} \sim \mathfrak{D}$,*

$$L_{\mathfrak{D}}(\mathbf{w}) \leq L_S(\mathbf{w} - \rho \mathbf{v}) + \sqrt{\frac{\dim(\mathcal{W}) \log \left(1 + \frac{\|\mathbf{w}\|_2^2}{\rho^2} \left(1 + \sqrt{\frac{\log(|\mathcal{S}|)}{\dim(\mathcal{W})}} \right)^2 \right) + 4 \log \frac{|\mathcal{S}|}{\delta} + \mathcal{O}(1)}{|\mathcal{S}| - 1}} + \mathcal{O}(\rho^3)$$

Proof *Using the bound from Lemma 2 we adapt the proof of Theorem 2 in Foret et al. (2021) (i.e. Eq. 13 and following) to show the claim.* \square

A.2 CURVATURE

We calculated the loss curvature in momentum direction, gradient direction and in random direction in Fig. A.1 if training with SGD, SAM and MSAM for WRN-16-4 on CIFAR100. For this we calculate $\epsilon^T \text{Hess}(L_S(\mathbf{w}))\epsilon$ for direction vectors ϵ (normalized to $\|\epsilon\|_2 = 1$) every 50 optimizer steps. The curvatures in momentum directions are larger than the curvature random direction (which tends towards the mean curvature as amount of parameters increase) for all optimizers and epochs, validating Setting 1 in Appx. A.1 and thus the suitability of momentum directions for sharpness estimation (especially compared to random perturbations; cf. Appx. A.7). Additionally, the curvature in these directions offers a measure for the loss sharpness. Since a local minimum of high curvature is approached, all three curvatures increase at the end of the training for SGD. Similarly to Fig. 4, SAM and MSAM are reducing the curvature best in their corresponding perturbation direction and MSAM yields lower curvatures than SAM in random directions.

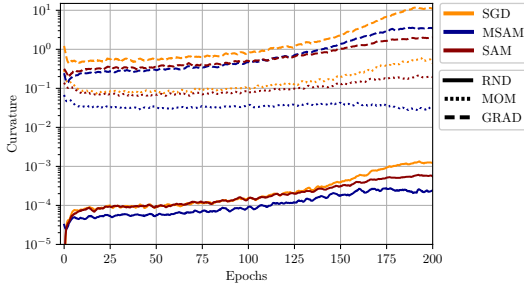


Figure A.1: Curvature of random directions (RND), momentum (MOM) and gradient (GRAD) for different optimizers.

A.3 EFFECTS OF MSAM/SAM DURING ViT’S WARM-UP PHASE

We further investigate the effect of SAM/MSAM during warm-up phase in Tab. A.1. As described above, we do not apply MSAM during the warmup phase by default (i.e. setting $\rho = 0$) since if doing so, we observe a drop in test accuracy from 69.1% to 66.1% which is below the AdamW baseline. We assume fluctuations of the momentum vector, that determines the perturbation direction for MSAM, to cause instabilities during the warmup phase. A similar effect can be seen for SAM, however, it is less pronounced, so that applying perturbations during the warm-up phase does not thwart SAM hugely. Since we focused on proposing a computationally more efficient variant and not on improving the generalization of SAM in this work, we thus decided to stay consistent with related work and conduct our extensive experiments in Tab. 2 while applying SAM also during the warm-up phase. Nevertheless, we would generally propose to apply SAM only after the warmup phase for ViT models to further improve SAM. We think further investigating effects of ρ -scheduling for SAM and MSAM is of high interest. E.g., Zhuang et al. (2022) investigated to reduce ρ during training (contrary to what our findings suggest) by binding it to the learning rate scheduling for SAM and they did not notice benefits. Despite the discussion in Sec. 4.4, we could not observe analogous effects for ResNets (though we did not study these extensively).

Table A.1: Impact of application of SAM/MSAM during warm-up phase. ViT S/32 on ImageNet. By default MSAM is applied after warmup phase only while SAM is always applied.

AdamW	SAM	SAM (after warmup only)	MSAM	MSAM (during warmup)
67.1	69.2	69.8	69.1	66.1

A.4 TRAINING AND IMPLEMENTATION DETAILS

If not stated differently, we calculate uncertainties of mean accuracies by 68% CI estimation assuming Student’s t-distribution.

We tuned weight decay and learning rates for our baseline models (SGD/AdamW) and did not alter

these parameters for the other used optimizing strategies. We used basic augmentations (horizontal flipping, cutout and cropping) for CIFAR100 trainings and normalized inputs to mean 0 and standard deviation 1. For ImageNet trainings we used Inception-like preprocessing (Szegedy et al., 2015) with 224x224 resolution, normalized inputs to mean 0 and std 1 and clipped gradients L2-norms to 1.0. We used ViT variants proposed by Beyer et al. (2022). A full implementation comprising all models and configuration files is available at <https://XXXXXXXX>.

Table A.2: Training Hyperparameters

	CIFAR100		ImageNet	
	WideResNets	ResNet50	ResNets	ViTs
Base Optimizer	SGD	SGD	SGD	AdamW
Epochs	200	200	100	90/300
Learning Rate	0.5	0.1	1	1e-3
LR-Scheduler	cos	cos	cos	cos + linear warm-up (8 epochs)
Label Smoothing	0.1	0.1	0.1	-
Batch Size	256	256	1024	1024
Weight Decay	5e-4	1e-3	1e-4	0.1

A.5 DETAILS ON OPTIMIZER COMPARISON

We report experimental details on the results presented in Tab. 1 in this section.

To calculate the speed, we conducted a full optimization on a single GPU for each model and dataset combination, normalized the runtime by SGDs runtime and report the average over all runs per combination.

We trained ViT-S/32 on ImageNet for 90 epochs for all models. Further hyperparameters not specific to SAM variants are reported above in Appx. A.4. Due to limited computational capacities and inline with related work, we did not perform runs for multiple random seeds for ImageNet trainings. Thus, we did not report standard deviations for these runs.

We adapted official implementations of ESAM (Du et al., 2022b) and MESA (Du et al., 2022a) while no official implementation was available for LookSAM (Liu et al., 2022).

For LookSAM, we fixed the trade-off parameter $k = 5$ and conducted a thorough search on the additional hyper parameter α , since the value suggested for ViTs by the original authors ($\alpha = 0.7$) was not suitable for our experiments (also see Fig. A.4). We decided to set $\alpha = 0.1$, while runs for $\alpha > 0.3$ did not yield further performance increases. Full hyperparameter search results are reported in Fig. A.2.

ESAM comprises two hyperparameter (γ and β) that steer the performance/runtime tradeoff which we set to match those of the original paper (i.e. $\gamma = \beta = 0.5$).

For MESA we tuned the regularization factor λ instead of the perturbation strength ρ .

Please also note the full ρ scan results presented in the next section (Fig. A.3 and Fig. A.4)

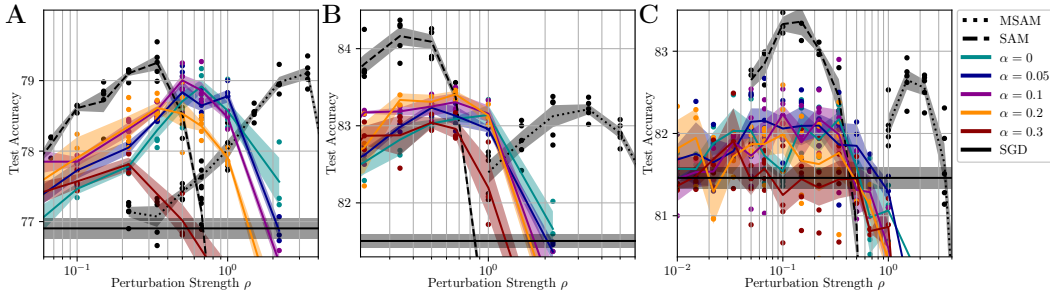


Figure A.2: Full results for ρ and α search for lookSAM ($k = 5$) on CIFAR100. Shaded cone: 68% CI. Dots: Random Seeds. A: WideResNet-16-4. B: WideResNet-28-10. C: ResNet-50.

A.6 FULL HYPER PARAMETER SEARCH RESULTS

We report our full ρ -hyperparameter search results in Fig. A.3, Fig. A.4 and Fig. A.5. In consistency with related work, we report results for best ρ only, in the main text. We sampled ρ with approximately even spacing on logarithmic scale with 6 datapoints per decade, i.e. $\rho \in \{\dots, 0.1, 0.15, 0.22, 0.34, 0.5, 0.67, 1, 1.5, \dots\}$, for experiments on CIFAR100 and with 4 datapoints per decade, i.e. $\rho \in \{\dots, 0.1, 0.17, 0.3, 0.55, 1, 1.7, \dots\}$, on ImageNet for experiments in Sec. 3. We used a slightly denser sampling for the visualizations in Sec. 4, but did not use those results for comparisons against baselines or other methods.

While optimal values for ρ vary slightly between models and datasets, we do not observe higher susceptibility to changes in ρ of MSAM compared to SAM.

Over all models and datasets we find higher optimal ρ values for MSAM compared to SAM. Perturbation vectors are normalized (L2-norm), so we conjecture components for parameters of less importance to be more pronounced for momentum vectors compared to gradients on single batches. For ViT models, we find optimal ρ values to be higher compared to ResNets. If chosen even higher, heavy instabilities occur during training, up to models not converging, limiting performances especially for MSAM. Similar to the observations during warm-up phase discussed above, this effect is more pronounced for MSAM. Notably, MSAM loses most performance against SAM on the biggest ViT models and if trained for 300 epochs, when highest ρ values are optimal for SAM. This suggests, that even better performances might be achievable for MSAM if the instability problems are tackled. Strategies to do so might include e.g. clipping ϵ or scheduling of ρ , which we intend to pursue in future work.

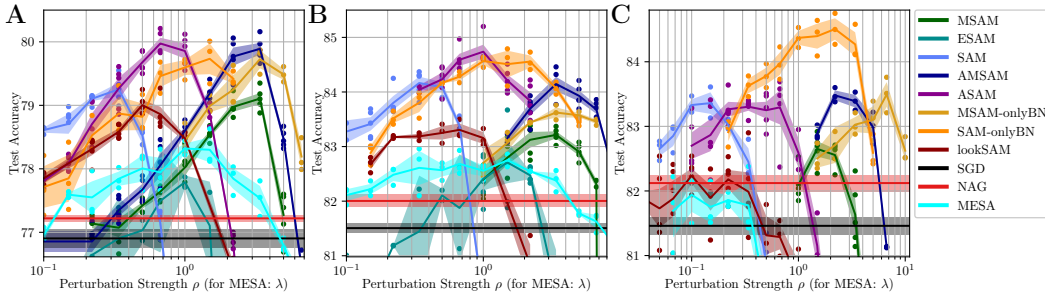


Figure A.3: Full results for ρ -search for different SAM/MSAM variants on CIFAR100. AM-SAM/ASAM refer to adaptive-MSAM/adaptive-SAM as in Kwon et al. (2021). For LookSAM we set $k = 5$ and report only the best performing value of $\alpha = 0.1$ (cf. Fig. A.2). For MESA: λ -search results plotted on same axis. Shaded cone: 68% CI. Dots: Random Seeds. **A:** WideResNet-16-4. **B:** WideResNet-28-10. **C:** ResNet-50.

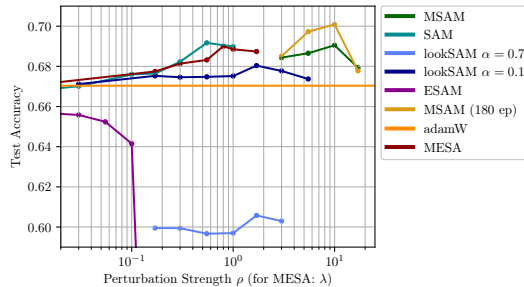


Figure A.4: Full results for ρ -search for different SAM/MSAM variants for ViT-S/32 trained for 90 epochs on ImageNet. For MESA: λ -search results plotted on same axis.

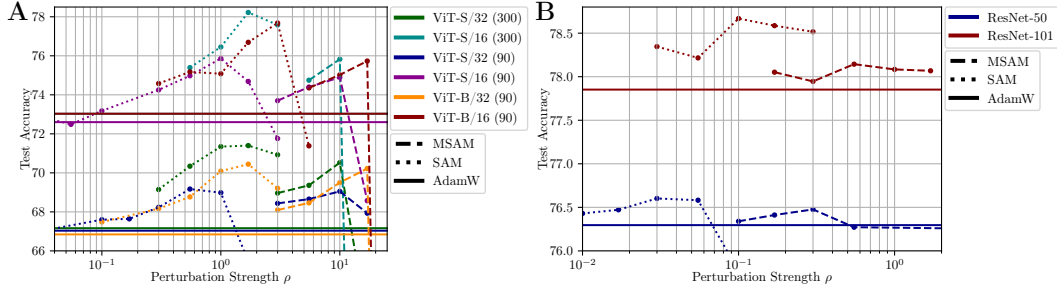


Figure A.5: Full results for ρ -search for all models tested on ImageNet (see Tab. 2). **A**: Vision Transformer (epochs in parentheses). **B**: ResNets.

A.7 RANDOM AND LAST GRADIENT PERTURBATIONS

Instead of the momentum vector v_t in MSAM, we also tried to use other perturbations ϵ which are independent of the current gradient and thus do not bring significant computational overhead, namely the last iterations gradients g_{t-1} (cf. Daskalakis et al. (2018); Lin et al. (2020a)) with positive and negative sign as well as Gaussian random vectors (cf. Wen et al. (2018)). For each variation, we tested absolute perturbations (Fig. A.6A)

$$\epsilon^{\text{ABS}} = \rho \frac{\delta}{\|\delta\|} \quad (10)$$

and relative perturbations (Fig. A.6B)

$$\epsilon^{\text{REL}} = \rho \frac{\delta|w|}{\|\delta w\|}, \quad (11)$$

with weights w (multiplied element-wise) and, e.g., $\delta = -v_t$ for MSAM. MSAM provides the only perturbation reaching SAM-like performance without inducing relevant computational overhead.

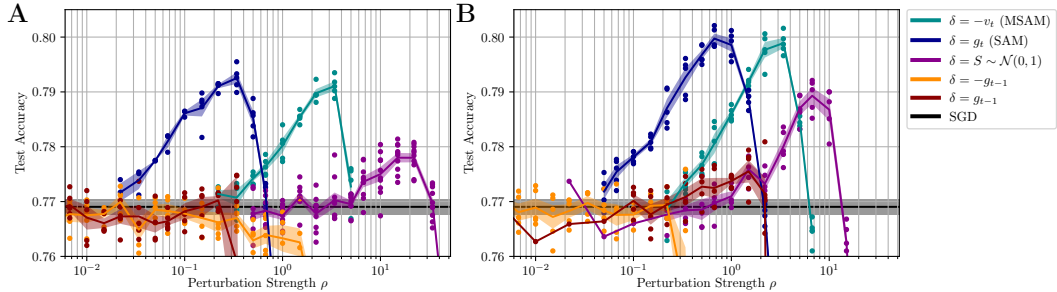


Figure A.6: Random perturbations and last gradient perturbations compared to SAM and MSAM. **A**: Absolute perturbations, **B**: Relative perturbations, i.e., scaled by $|w_i|$ before normalization. All perturbations normalized by L2-norm and scaled by ρ . WideResNet 16-4 trained on CIFAR100. MSAM always better than other current gradient-independent perturbations.

A.8 HYPERPARAMETER STABILITY

To show the stability of MSAM and its hyper parameter ρ , we varied the learning rate η and the momentum factor μ when optimizing a WRN-16-4 on CIFAR100 for fixed $\rho = 2.2$ and depict results in Fig. A.7. MSAM yields stable performance increases compared to SGD and NAG over wide ranges of hyperparameters. We made similar observations when comparing SGD and MSAM for different number of epochs (cf. Fig. A.8).

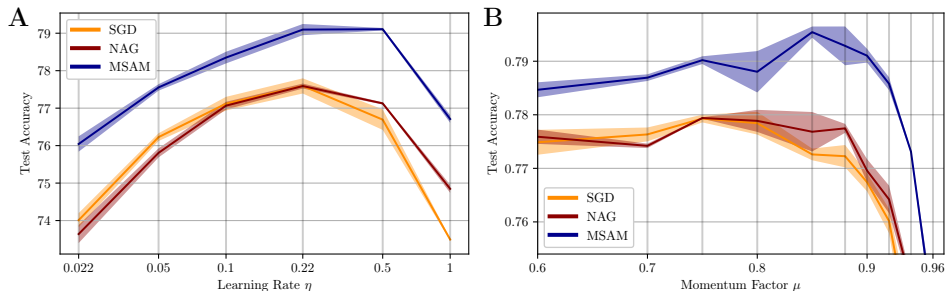


Figure A.7: WRN-16-4 on CIFAR100 fixed $\rho = 2.2$. A: Learning rate η ablation (log-scale). B: Momentum factor μ ablation.

A.9 COMPARISON WITH SAME COMPUTATIONAL BUDGETS

We compare MSAM and SAM (and SGD and NAG) when given the same computational budget for WRN-16-4 on CIFAR100 for a wider range of epochs (up to 1200) in Fig. A.8. I.e., running SAM for half the number of epochs compared to other optimizers, resulting in the same number of network passes for all optimizers. MSAM performs similar to NAG (and SGD) for short training times, however, if trained until convergence of SGD/NAG or even longer (overfitting occurs; SGD/NAG results decrease again) MSAM reaches higher test accuracies and overfitting is prevented. Due to the additional forward/backward passes SAM performs worse compared to MSAM for limited computational budgets. For long training times MSAM and SAM do not differ significantly. We further support these observations by training a ViT-S/32 with MSAM with doubled number of epochs (180) on ImageNet where we reach 70.1% test accuracy and thus clearly outperform SAMs 69.1% (cf. Tab. 2).

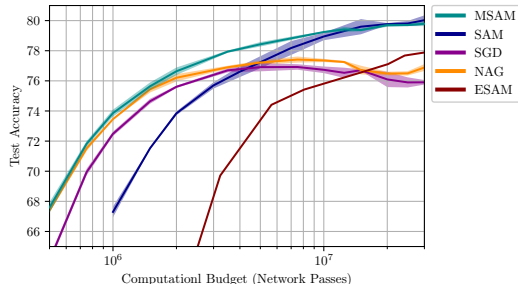


Figure A.8: Comparing different optimizers when given the same computational budget. WRN-16-4 on CIFAR100.

A.10 MACHINE TRANSLATION

Machine translation results (English to Romanian) on the WMT 2016 (Bojar et al., 2016) dataset by finetuning a T5-tiny model (efficient version by Tay et al. (2022)) from a publicly available checkpoint pretrained on the C4 dataset (Raffel et al., 2019). We scanned $\rho \in \{0.01, 0.03, 0.1, 0.3, 1\}$ and found MSAM and SAM both to perform best at $\rho = 0.1$. The resulting BLEU scores are shown in Tab. A.3. MSAM slightly outperforms SAM (as well as AdamW) while requiring two times less computations.

Table A.3: BLEU scores for T5-tiny trained on English to Romanian translation on the WMT 2016 dataset.

AdamW	SAM	MSAM
23.35	23.57	23.64

A.11 LOSS ASCENT IN MOMENTUM DIRECTION

To validate that the perturbation of the loss results in a loss increase, we show the perturbed and unperturbed loss during training for different learning rates in Fig. A.9.

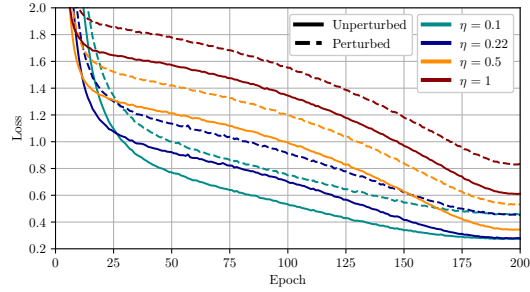


Figure A.9: Loss before ($L_{\mathcal{B}_t}(\mathbf{w}_t)$) and after ($L_{\mathcal{B}_t}(\mathbf{w}_t - \rho \mathbf{v}_t / \|\mathbf{v}_t\|)$) perturbation in momentum direction as done by MSAM ($\rho = 3$) for WRN 16-4 on CIFAR100 for different learning rates.